Miniature TL-based RF Tracking Devices for Prospective Motion Correction in MRI at 7 T

Aleksandra Sulikowska, Andrew M. Peters, Penny A. Gowland, Paul M. Glover

Sir Peter Mansfield Magnetic Resonance Centre, University of Nottingham, Nottingham, NG7 2RD, United Kingdom

Target Audience: Researchers interested in new hardware solutions for prospective real-time correction for head motion in high field MRI.

Purpose: Various techniques have been proposed to compensate for image artefacts caused by subject motion during MR brain imaging. Retrospective approach to the problem have been explored in detail and widely applied in neuroscience research and clinical applications[1-3].The prospective real-time approach, is however, relatively new and various interesting hardware solutions have been proposed[4-6]. Here we present a prototype of an innovative external tracking system employing miniature self-screened transmission-line (TL) based devices, which can be used for prospective motion correction of brain imaging at 7 T. The system we propose has a number of advantages discussed here. We show the preliminary position measurements and some of the further development ideas.

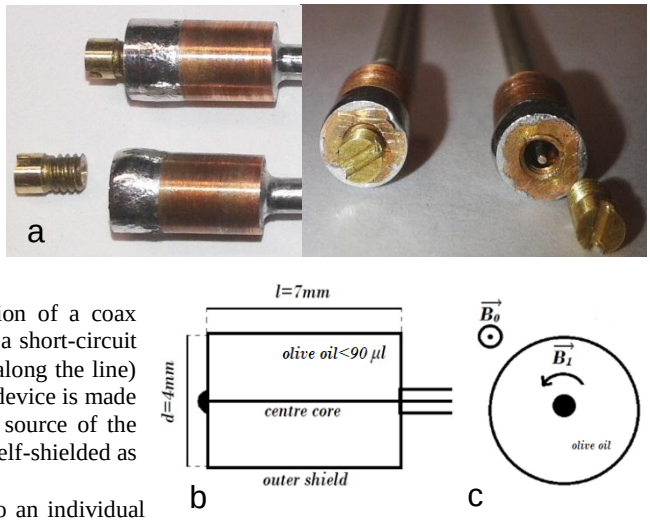

Fig.1. *Prototype TL-based RF tracking device;* ***a****: Photographs.* ***b****: Schematic internal-section.* ***c****: Schematic cross-section; l-length, d-internal diameter.*

Methods: The prototype single tracking device is built as a short extension of a coax transmission-line (7 [mm] length). As the TL is effectively terminated with a short-circuit and has a total length (l) of $0 < l \ll \lambda/4$ (where λ is a voltage wavelength along the line) the input impedance of the TL is considered to be inductive. The TL tracking device is made of copper with an insulating layer being an olive oil sample, which is the source of the signal. The TL device works in both transmitting and receiving modes and is self-shielded as the RF magnetic field is enclosed inside the device.

The whole tracking system consists of 5 TL devices, each connected first to an individual tuning and matching circuit and second to the control circuit board. The control circuit board works as a T/R switch (by employing pin diodes and $\lambda/4$ length cables), splits the signal from Philips transmitter between 5 TL devices (employing simple resistor splitting as only a low power of a few [mW] is required for the RF pulses) and connects the 5 TL devices to 5 (out of 32) channels of the Philips multi-channel receiver box. The TL devices are intended to be attached to a wearable frame on the head eventually but are clamped to a moveable jig for these experiments.

Position data from one of the 5 tracking devices was acquired on 7 T Philips Achieva Scanner (Philips Medical Systems, Best, The Netherlands). A 4-pulse-acquire readout sequence was implemented into Philips Software to obtain the FID under each of the three orthogonal gradient directions with the fourth acquisition without gradient projection added for B_0 drift correction. The frequency was calculated for each acquisition and the location of the TL device $\vec{r} = (r_x, r_y, r_z)$ [m] was determined uniquely in the 3-D scanner coordinate system using the relationship $r_{x,y,z} = f_{x,y,z} / \gamma / G_{x,y,z}$ [m] ($G_{x,y,z}$ [T/m] is the gradient amplitude). The accuracy of measurements was evaluated using a non-magnetic platform installed inside the scanner bore to provide a framework for reproducible movement in 3 orthogonal gradient directions (platform accuracy < 0.001 [mm] measured with dial indicator). Spatial coordinates of the device were calculated as mean values from 20 measurements in each position (10 distances measured).

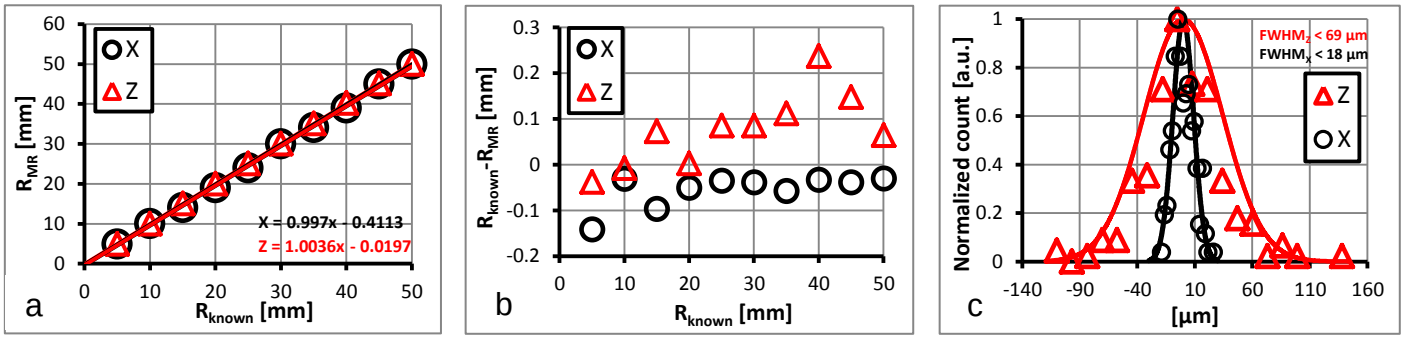

Fig. 2*.* ***a****: Accuracy of measurements displayed as a comparison between R_{MR} and R_{known}.* ***b****: Measurement error represented as R_{known} -R_{MR} vs. R_{known}.* ***c****: Reproducibility of MR position measurements with Gaussian fitting.*

Results: A 90 degree 100 microsecond pulse could be obtained with only a few [mW] of RF power. The FID had an SNR typically > 1000. Due to similarity of the physical *X*- and *Y*- gradients, behaviour in the *Y*- direction was not presented here. The accuracy of MR measured distances (R_{MR}) with respect to platform measured distances (R_{known}) is shown in ***Fig. 2a.*** Linear fitting parameters are shown on the graph. Better visualization of the small errors is presented in ***Fig. 2b*** as R_{known}-R_{MR} vs. R_{known}. Localization errors (mean absolute value of R_{known}-R_{MR} ± std) were calculated as 0.06 ± 0.04 [mm] and 0.09 ± 0.07 [mm] along the *X*- and *Z*- direction. Reproducibility of the position measurements is presented as the standard deviations ($std_{x,z}$) of each R_{MR} (20 measurements for each R_{MR}) and for clarity presented in ***Table 1***. Reproducibility of the position data is also shown in ***Fig. 2c*** in form of a histogram of the deviation of each measurement from its corresponding mean and depicts Gaussian distribution with full-width at half-maximum FWHM < 18 [µm] and < 69 [µm] for *X*- and *Z*-direction, indicating high measurement precision.

R_{MR} [mm]	Std_x [mm]	Std_z [mm]
5	0.013	0.048
10	0.009	0.058
15	0.012	0.028
20	0.008	0.039
25	0.009	0.034
30	0.011	0.012
35	0.009	0.061
40	0.008	0.026
45	0.008	0.011
50	0.009	0.019

Table 1. The std of each measured distance (R_{MR}).

Discussion: A novel design of a tracking NMR device has been demonstrated to be suitable for real-time motion correction. The small TL-based NMR device is a transmitter and receiver with integrated olive oil sample and RF magnetic field enclosed inside the probe. The device works independently to the image acquisition process, allowing the use of high flip angles of an RF-pulse and is expected not to interfere with the image data. The experiments demonstrate preliminary position tracking results and show high reproducibility of measurements and accuracy of the device.

References: **1.** Glover et al. MRM 44:162-167, **2.** Ehman et al. Radiology 173:255-263, **3.** Johnson et al. Magn. Imag. 30:655-665 69:734-748, **4.** Ooi et al. MRM 62:943-954, **5.** Quin et al. MRM 62:924-934. **6.** Zaitsev et al. Neuroimage 31:1038-1050.